Nano Energy 58 (2019) 641–651

Contents lists available at ScienceDirect

Nano Energy

journal homepage: www.elsevier.com/locate/nanoen

Full paper

Self-powered glove-based intuitive interface for diversified control applications in real/cyber space

Tianyiyi He[a,b,c,d,1], Zhongda Sun[a,b,c,d,1], Qiongfeng Shi[a,b,c,d,1], Minglu Zhu[a,b,c,d], David Vera Anaya[f], Mengya Xu[a,c,d], Tao Chen[e,*], Mehmet Rasit Yuce[f], Aaron Voon-Yew Thean[a,c], Chengkuo Lee[a,b,c,d,**]

[a] Department of Electrical & Computer Engineering, National University of Singapore, 4 Engineering Drive 3, Singapore 117583, Singapore
[b] National University of Singapore Suzhou Research Institute (NUSRI), Suzhou Industrial Park, Suzhou 215123, China
[c] Hybrid Integrated Flexible Electronic Systems (HiFES), National University of Singapore, Block E6 #05-3, 5 Engineering Drive 1, Singapore 117608, Singapore
[d] Center for Intelligent Sensors and MEMS, National University of Singapore, Block E6 #05-11, 5 Engineering Drive 1, Singapore 117608, Singapore
[e] Jiangsu Provincial Key Laboratory of Advanced Robotics, School of Mechanical and Electric Engineering, Soochow University, Suzhou 215123, China
[f] Department of Electrical and Computer Systems Engineering, Monash University, 14 Alliance Lane, Clayton, Victoria, Australia

ARTICLE INFO

Keywords:
Human machine interface
Triboelectric nanogenerator
Self-powered sensor
Virtual reality
Augmented reality

ABSTRACT

Present Human Machine Interfaces (HMIs) that vary in shapes, operation schemes, and functions can be frequently found in our daily life, and the giant market demand has been pushing the development of the HMIs since the last decades. To greatly extend the communication channels between humans and external devices in a natural way, here we report an intuitive, self-powered, low-cost, and glove-based HMI towards diversified applications. A minimalist design based on the triboelectric nanogenerators (TENG) in two configurations is proposed to balance the requirement on the full functionality and the simplified signal processing capacity of the HMIs. Each TENG sensor is composed of a PEDOT:PSS coated textile strip stitched onto the glove and a layer of silicone rubber thin film coated on the glove. The glove-based interface has been successfully demonstrated for wireless car control, wireless drone control, minigame control, VR game control, and cursor control for online shopping as well as alphabet writing with a simple and intuitive operation technique. This glove-based interface provides a novel minimalist design concept distinct from the present rigid and bulky HMIs to open up a new direction of the further development of the HMIs with advantages of flexibility/wearability, low cost, easy operation, simplified signal processing, and low power consumption.

1. Introduction

The Internet of Things (IoT) has become a dominating trend with industrial and consumer products being connected via the internet. To operate these devices, Human Machine Interfaces (HMIs) are becoming an essential part for the further development of the IoT [1]. Flexibility and wearability of the HMIs, as a crucial property for the HMIs to be carried by humans in a comfortable and simple way, has become an research challenge that draws massive attention from diversified areas to conquer the barrier between the flexibility and the similar performance compared to rigid sensors with varying sensing capabilities [2–4]. Accordingly, significant efforts have been made recently including the development of stretchable conductors [5,6], flexible/stretchable semiconductors [7], highly sensitive physical sensors [8–11], multifunctional electronic skin [12], etc. Although the power consumption for each device in the HMIs may be small, the quantity of the sensor nodes in the sensor network could be massive which could lead to a large energy expenditure over time [13]. In addition, the optical sensor interacting system that remotely detects human motions by image recognition become one of the mainstream technologies in quite a few applications [14]. However, this kind of technologies requires a powerful computing capacity either from the device itself or the Cloud server, which brings in sizable power consumption to the whole system. To address these issues, self-powered sensors based on

* Corresponding author.
** Corresponding author at: Department of Electrical & Computer Engineering, National University of Singapore, 4 Engineering Drive 3, Singapore 117576, Singapore.
E-mail addresses: chent@suda.edu.cn (T. Chen), elelc@nus.edu.sg (C. Lee).
[1] These authors contributed equally.

https://doi.org/10.1016/j.nanoen.2019.01.091
Received 10 December 2018; Received in revised form 2 January 2019; Accepted 22 January 2019
Available online 01 February 2019
2211-2855/

the mechanism of piezoelectric [15–19], electromagnetic [20,21], and triboelectric [22–25] have been massively developed. Recently, Chen et al. reported a simple design with only four outputs to realize a wearable sensing patch as a 3D motion control interface for a robotic manipulator, showing an interesting and energy-compatible HMI solution [26]. Moving forward, this kind of minimalist design to provide sensing functions in an energy-compatible HMI could be a new strategy for the implementation of a user-friendly HMI in near future.

Most of the HMIs such as keyboard only require a digital control where only state “0” and state “1” are involved [27,28]. In some special cases, one or two more states are also demanded to fulfill a more sophisticated control. In general, sensors that are able to monitor a continuous human motion are not necessary for the majority of the HMIs to implement the desired functions from users. Besides, it is difficult to produce a precise force or bending angle for the control system by different users. Instead, a minimalist design that exactly balances the requirement on the easy operation and the full functionality is highly desired. Especially, a wearable HMI with a complicated sensing mechanism or structure is almost impossible to be a perfect fit for every user due to the physical difference between each individual, which may lead to a great complexity for the sensors to be calibrated and for the users to learn the operation techniques especially for the elderly and the child. Consequently, there is an immense demand for the development of a fully functional, power-compatible, and user-friendly HMIs.

As a common wearable item, glove is closely related to human's daily life and human fingers are one of the most flexible and dexterity body parts, which is a perfect fit for a substrate of the HMIs [29,30]. Textile, due to its unique properties of soft nature, wearable convenience, light-weight, natural micro-structure, and air permeability, has been demonstrated to be an ideal material for varying wearable applications [31–37]. Thus, using the finger bending motions as well as the contact motions between adjacent fingers to realize a 2D control is one of the simplest and the most intuitive approaches that perfectly fits the brain logic. Piezoresistive sensors [38], which is one of the most common methods to measure force and strain, is not a preferential choice for this kind of applications since it requires a power supply to function. Similarly, piezoelectric-based self-powered sensors have also been demonstrated to be an alternative choice for both strain and force measurement [39–43]. However, the common and commercialized piezoelectric materials that can provide a considerable output are mostly ceramic-based hence rigid [44]. Besides, the further advancement of the flexible piezoelectric sensor still faces challenges making its way to large-scale production for practical use due to the sophisticated fabrication process and the smaller output than the rigid ceramics [45,46]. Triboelectric nanogenerator (TENG), owing to its unique advantages of sizeable output, diversified choice of materials, easy fabrication, lightweight, simple working mechanism, and low cost, could be an optimal option for a glove-based intuitive HMI with a minimalist design [47–56].

Herein, we propose a glove-based and self-powered intuitive human machine interface towards diversified applications including 2D control, 3D control, cursor control, and game control as illustrated in Fig. 1(a). The present control interfaces such as all kinds of joysticks, the mouse, or the keyboard, are all rigid, bulky, and time-consumable to get familiar with the operation techniques. To realize an intuitive and user-friendly control, we incorporated the PEDOT:PSS coated textiles that are fabricated with a low-cost dip coating approach and the silicone rubber painted on the glove outer surface into a cotton glove through a minimalist design. This glove-based interface provides a brand new intuitive and self-powered control technique to the users in a wide range.

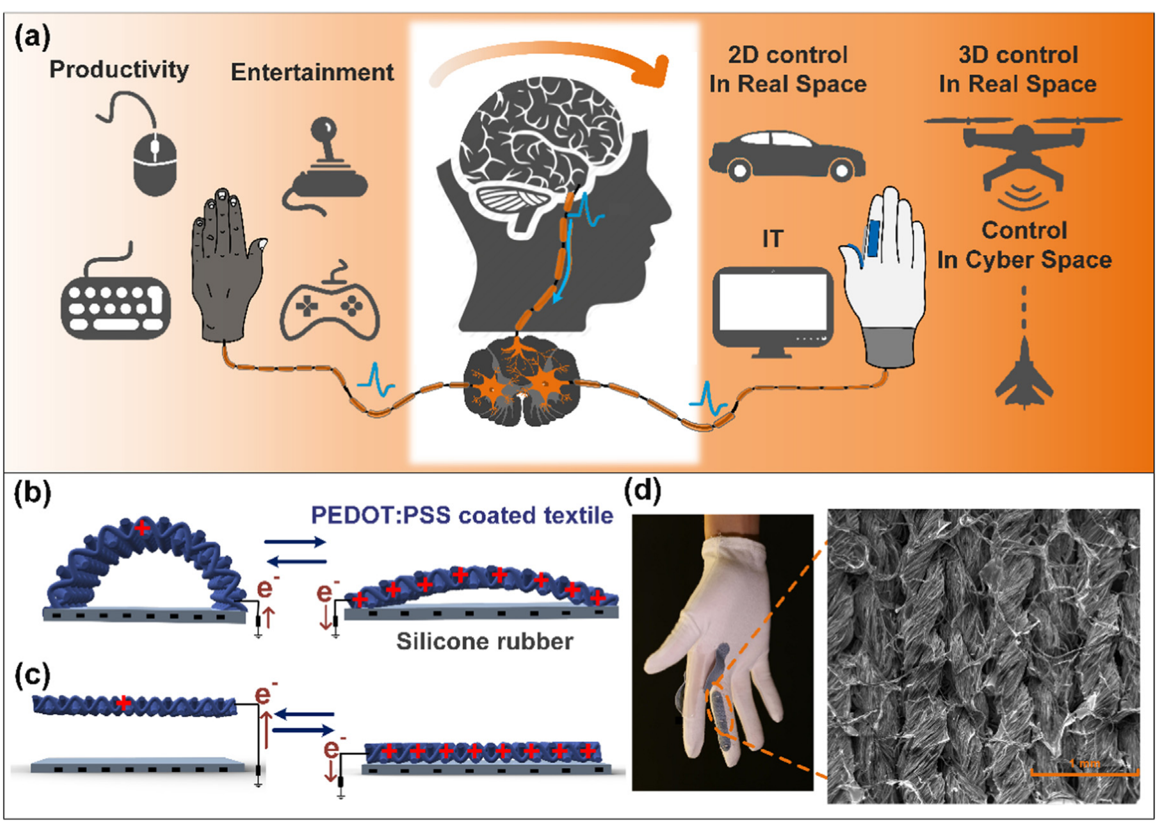

Fig. 1. (a) Schematic drawing showing the control flow of a subject during the interactions with diversified machines through traditional control interfaces and the intuitive glove-based interface. (b) The working mechanism of the arch-shaped TENG under the stretching and releasing state. (c) The working mechanism of the contact-separation TENG sensor. (d) Photograph of the glove-based interface. Inset shows the SEM image of the PEDOT:PSS coated textile.

2. Device design and characterization

Poly (3,4-ethylenedioxythiophene): poly (styrene sulfonate) (PEDOT:PSS) is one of the most successful conducting polymers which possesses multiple unique characteristics such as good physical and chemical stability in the air, superior optical transparency in visible light range, high electrical conductivity, good film-forming ability by versatile fabrication techniques, and availability of low-cost commercialized dispersion [57,58]. A fabric-based TENG composed of conductive textiles which were coated with metal Ni was reported by Pu et al. [59]. And coating the carbon nanotubes or the graphene on a textile substrate have also been reported recently [60,61]. Compared to metal Ni or the allotropes of carbon, PEDOT:PSS is much more suitable for wearable applications due to the aforementioned superior properties. Besides, Ding et al. have demonstrated the feasibility of fabricating a conductive textile by simply soaking the commercialized textile into the PEDOT:PSS solution [62]. Hence this facile and low-cost PEDOT:PSS coating approach is adopted to fabricate the conductive part in the cotton glove. The SEM image of the PEDOT:PSS functionalized textile is shown in Fig. 1(d).

For a 2D control interface, four basic directional controls are essential. Since fingers are one of the most flexible and dexterity body parts, to realize an intuitive control, four motions of the index finger including bending down at proximal interphalangeal (PIP) joint,

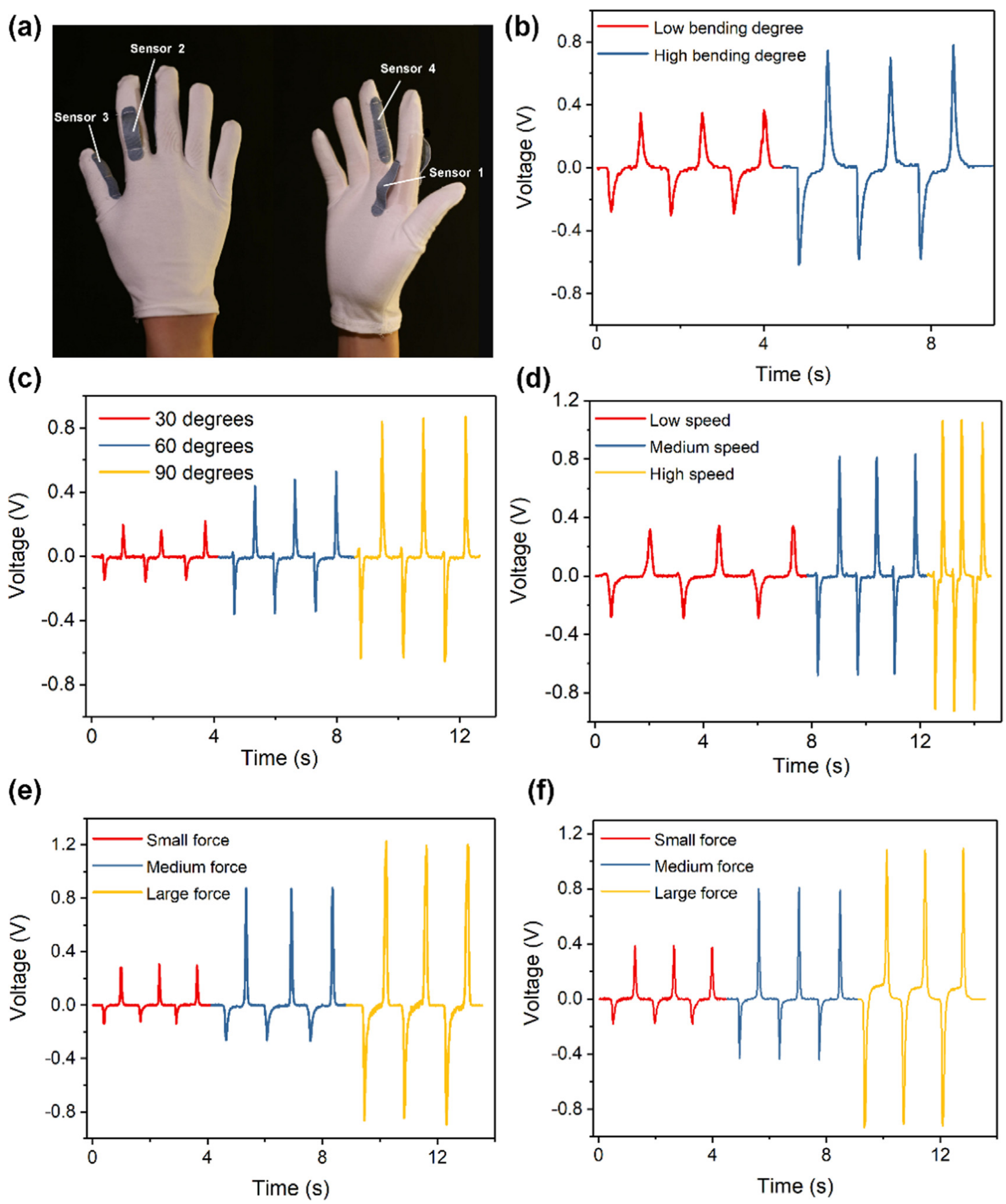

Fig. 2. Characterization of the four sensors. (a) Photographs with a front view and a side view demonstrating the configurations and the positions of the four sensors. (b) The real-time output of sensor 1 when the index finger bends up at a low degree and a high degree with a constant speed. (c) The real-time output of sensor 2 when the index finger bends downs at 30 degrees, 60 degrees, and 90 degrees at a same speed. (d) The real-time output of sensor 2 when the index finger bends downs at 90 degrees at different speed. (e) The real-time output of sensor 3 when the index finger contact with the thumb with an ascending applied force. (f) The real-time output of sensor 4 when the index finger contact with the middle finger with an ascending applied force.

bending up at the metacarpophalangeal (MP) joint, contacting with the side of the thumb, and contacting with the middle finger are endowed with four direction moving commands towards different applications. Moving the index finger to contact with the adjacent fingers on its left and right side can be easily associated with the left and right movements of the controlled objects. The process of bending the index finger at the PIP joint is akin to a forward or downward arrow as shown in Fig. S1 (a), which is highly synchronized with the moving direction of the controlled object (forward or downward). Similarly, the bending direction of the MP joint which is perfectly opposite to the one of the PIP joint as shown in Fig. S1 (b), corresponding to the moving backward or upward of the controlled objects. Accordingly, the four movements of the index finger are in good correspondence with the control commands in human instinct, which should largely reduce information processes during the whole control procedure.

Here we propose a minimalist design of a self-powered interface based on a cotton glove with four textile-based TENG sensors incorporated as shown in Fig. 2(a). To endow the glove-based interface with the functionality of the four-movements sensing, versatile structures of the TENG could be implemented. Pu et al. reported a triboelectric quantization sensor with a high resolution for rotation sensing as well as bending sensing of a finger with the sliding-structure TENG [63]. But the majority part of the device is still rigid, and such high resolution for the targeted control scenarios of this glove-based interface is not essential. Hence, to realize a fully flexible and stretchable HMI with a minimalist design that can satisfy the sensing requirement, two different kinds of sensor configurations are proposed with the same triboelectric materials as shown in Fig. 1(b–c) based on the required command gestures. In Fig. 1(b), the arch-shaped textile-based sensor is implemented to measure the finger bending motions, while the configuration in Fig. 1(c) is to detect the contacts between the index finger and its adjacent fingers. The working mechanisms for all the TENG sensors are based on the contract-separation mode of the TENG as shown in Fig. 1(b–c) in order to simplify the interface structure as much as possible. The photos of the four sensors incorporated into the sensing glove are shown in Fig. 2(a), which are labeled from 1 to 4 based on the endowed function. Before stitching the PEDOT:PSS coated textiles on the glove, a thin layer of silicone rubber was painted onto the four sides of the index finger where the contact-separation processes happen. The contact separation sensor is 1 cm wide and 4 cm long that perfectly fits even a small finger. And the arch-shaped sensor is 1.3 cm wide and 4 cm long with an arch height of 6 mm.

Four sensors are characterized separately under different finger motions. Each conductive textile strip is connected out to a commercialized Microprogrammed Control Unit (MCU) from channel 1 to channel 4 for signal acquisition which is then connected to a computer for real-time display. Firstly, the index finger was controlled to bend up at the MP joint at a constant frequency of 1 Hz. This up bending motion will only trigger sensor 1 that is attached to the edge of the palm and the bottom end of the index finger, which could be defined as the up-movement control sensor accordingly. At a large bending angle around 60 degrees where the bending limit of the MP joint is, the collected negative voltage is at a large value of 0.6 V with a small variation of 0.03 V, while the negative voltage reaches its minimum value of −0.3 V with a variation of 0.05 V when the MP joint only bends slightly at around 30 degrees as shown in Fig. 2(b). The corresponding short-circuit current signal is given in Fig. S2(b). Similarly, the index finger is controlled to bend down at the PIP joint solely at 30 degrees, 60 degrees, and 90 degrees at a constant frequency of 1 Hz, and the real-time outputs from sensor 2 that is triggered individually in three cycles at each bending degree are depicted in Fig. 2(c), and its corresponding short-circuit current signal is given in Fig. S2(a). Since the position and the movement of sensor 2 are just reversed from that of sensor 1, sensor 2 could be defined as the down-movement control sensor appropriately. It can be observed that the output voltage increases with the bending angles, and hence the angle of the bending could be a variable parameter for a more sophisticated control in an intuitive way. The resistance change of the textile during the repetitive stretching-releasing process is given in Fig. S3. The overall resistance variation of the 1 cm × 4 cm textile strip is much smaller than its original resistance, and the impedance of the TENG is usually in MΩ scale. Hence the influence of the resistance change of the conductive textile on the triboelectric output can be negligible. Except for the bending angle, the speed of the movement will also affect the output of the finger bending sensor. As shown in Fig. 2(d), a higher speed of the bending motions gives rise to a higher output when the bending angles stay the same at 90 degrees. The low speed is around 0.138°/ms (± 0.014°/ms), the medium speed is around 0.287°/ms (± 0.04°/ms), and the high speed is around 1°/ms (± 0.125°/ms). To eliminate the interference between the two parameters, a medium moving frequency of 1 Hz is used for all the characterizations of the four sensors. The remaining two contact-separation sensors in charge of the movements perpendicular to the moving trajectory controlled by the arch-shaped sensors are characterized under different forces at a constant speed. A flexible commercial force sensor is used for precise calibration of the applied pressure. The triboelectric outputs of sensor 3 and sensor 4 under repetitive contact-separation processes at three-level applied forces are depicted in Fig. 2(e–f). The measured three-level forces are 0.8 N, 4 N, and 8 N respectively with a variation of 0.5 N. The corresponding current signals of them are given in Fig. S2(c–d). Similarly, the triboelectric outputs of the contact separation sensors increase with the applied force, which could be another control parameter to broaden the functionality of the glove-based interface for some special scenarios. To investigate the effect of the applied force on the triboelectric output of the textile-based TENG, a 2 cm × 2 cm textile-based contact-separation TENG is tested under different force load from 1 N to 27 N with a frequency of 2 Hz. The measured open-circuit voltage is depicted in Fig. S4. It can be observed that the output voltage increases with the applied force linearly in two regions, and it saturates at around 25 N.

Since this glove-based HMI is targeted for game control, here we define the response time of the TENG sensors as the time from the index finger starts to move to where the peak voltage is generated. For the triggering motion, it takes time for the finger to be at the position where the textile contacts with the silicone rubber, hence a mechanical switch is implemented here as a reference of the time where the finger starts to move. For the releasing motion, once the finger moves, the textile and silicone rubber start to separate, where only a negligible delay between the movement of finger and the signal generation is observed. In this case, the response time associated with the speed of the finger movement is studied in Fig. S5. A pair of the contact-separation sensor and the arch-shaped bending sensor are characterized individually. From slow motion to fast motion, the response time of the bending sensor varies from ~84 ms to ~230 ms for triggering and ~78–110 ms for releasing. While for the contact-separation sensor, the response time varies from ~96 ms to ~260 ms for triggering and ~63 ms to ~107 ms for releasing. It can be observed that the variation of the response time in releasing state in much smaller than the one in triggering state when different speed is applied. The durability of the two sensors is also tested as shown in Fig. S6. It can be observed that the triboelectric output voltage of the contact-separation sensor only shows a slight degradation of around 5% after being hit at 60 N for around 11,250 times. An arch-shaped sensor with a length of 4 cm and width of 1 cm is attached to a linear motor for repetitive stretching-releasing processes. After ~20,571 times of the stretching and releasing process, its triboelectric output voltage still maintains 97% of its original value. Both of the results demonstrate the good durability of the textile-based sensors. The tight adhesion between the PEDOT:PSS and the textile is further proved by the washability test in Fig. S7.

3. Game control in cyber space

To demonstrate the functionality of the glove-based and self-

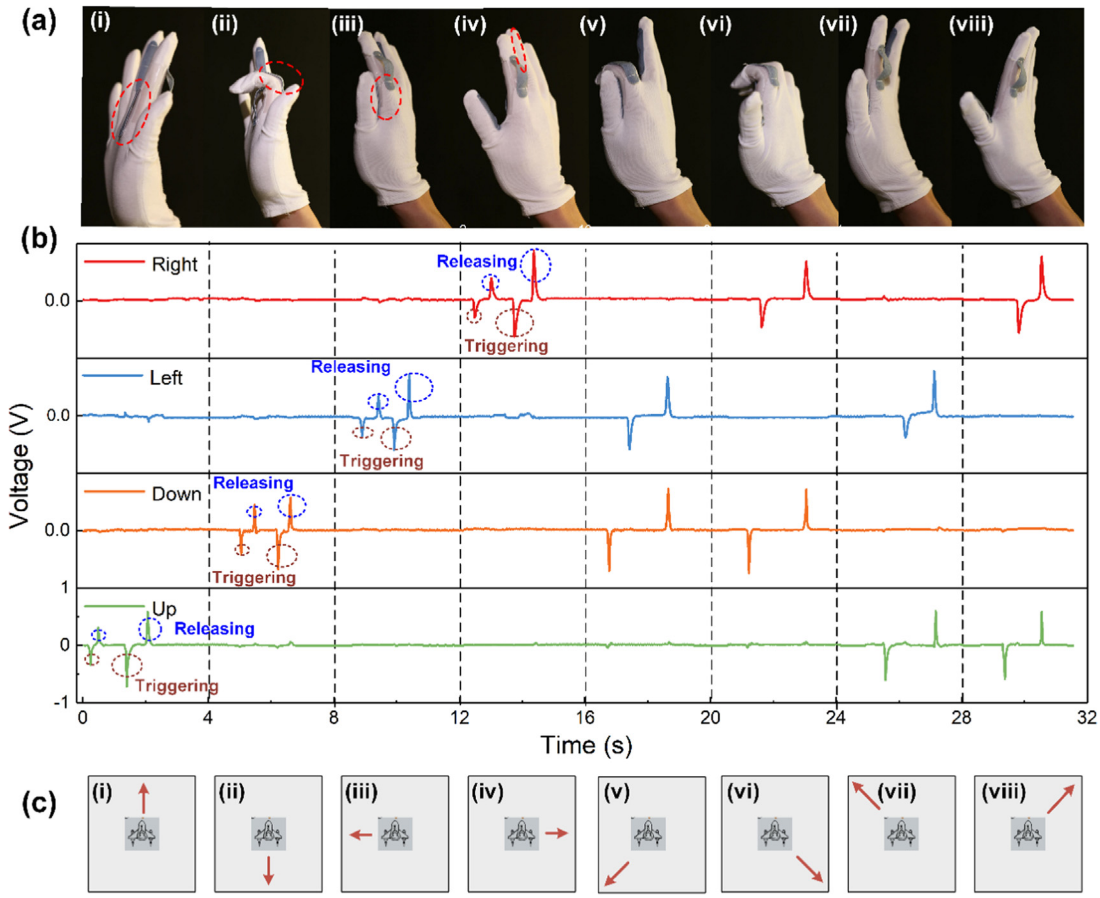

Fig. 3. Minigame control with the glove-based interface. (a) Eight hand gestures corresponding to the eight movements of the aircraft in the minigame. (b) The real-time outputs of the four sensors divided into eight segments corresponding to the eight hand gestures. (c) Pictures showing the eight-direction movements of the aircraft in the minigame triggered by the eight different gestures.

powered interface, the sensor outputs are implemented to control an aircraft move around in a shooting minigame on a computer. A video demo of the shooting minigame control can be found in Video S1 (Supporting Information). The operation technique of this minigame is to control the aircraft to move within the screen to shoot down as many enemy planes as possible. The four sensors from 1 to 4 are defined as the up-movement sensor, down-movement sensor, left-movement sensor, and right-movement sensor respectively in this specific application. Eight moving directions are allowable through controlling the TENG sensor-embedded glove: up, down, left, right, down left, down right, up left, and up right. The corresponding hand gestures performed to trigger the eight different moving signals are shown in Fig. 3(a). When the index finger bends up at the MP junction as shown in Fig. 3(a–i), sensor 1 located at the edge between the palm and index finger will generate a negative peak voltage due to the induced contact between the PEDOT:PSS coated textile and the silicone rubber thin film on the glove as shown in Fig. 3(b) and hence it will trigger the aircraft to move up at a constant speed. The aircraft stops moving when the index finger returns to its original position where a positive peak voltage (the releasing signal) is generated due to the separation between the PEDOT:PSS coated textile and the silicone rubber thin film. Similarly, sensor 2, sensor 3, and sensor 4 command the aircraft to move down, left, and right when the index finger bends down at the PIP joint, contacts with the side of the thumb, or contacts with the side of the middle finger. All the negative peak voltages generated due to the contact between the PEDOT:PSS textile and the silicone rubber thin film are triggering signals for the corresponding movements, and all the positive peak voltages are commands to stop the moving aircraft. Since the speed variation for this kind of minigame is not necessary, the hand gestures can be performed at any speed and force as long as the sensors being triggered. Additionally, diagonal movements are also possible when the two corresponding sensors are triggered during the same time period as shown in Fig. 3(a–v)-(a-viii). In general, this glove-based interface is able to function as a wearable game control interface for various minigames where just a 2D movement control is needed. The operation method is highly intuitive by only controlling the index finger to bend up, bend down, move left, and move right, which is easy to learn and use in a short time. Another video of a virtual reality (VR) automobile game control with the glove-based interface can be found in Video S2 (Supporting Information).

Supplementary material related to this article can be found online at doi:10.1016/j.nanoen.2019.01.091.

4. Wireless car control and drone control

As what has been demonstrated in the sensor characterization part, the outputs of the sensors can be controlled by the applied force or the bending angles, which could provide more states than the state “0” and state “1” in the minigame control. To demonstrate a more advanced and complicated control, the glove-based interface is implemented to manage a toy car wirelessly. The circuit connection for the wireless car control is depicted in Fig. 4(a). The four sensors are connected to an MCU through a processing circuit that eliminates environmental noise and minimizes the possible interferences between different channels. In this scenario, the triboelectric outputs from the sensor 1–4 are defined as commands of running backward, running forward, turning left, and turning right. The outputs of the sensors are connected to one MCU for signal acquisition and processing to decide the corresponding control

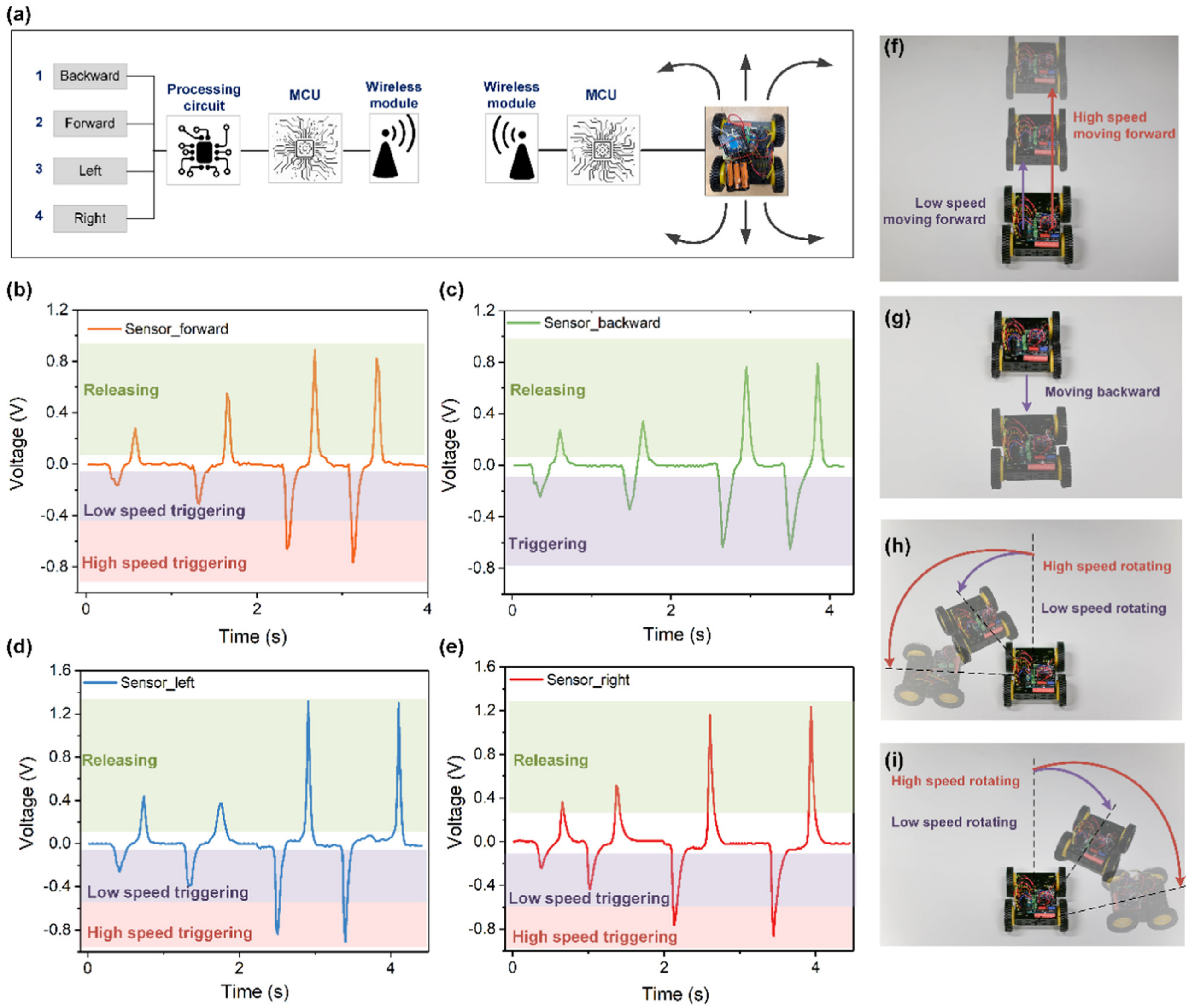

Fig. 4. Wireless car control with the glove-based interface. (a) Schematic diagram showing the circuit connection from the sensors on the glove to the toy car. (b) The real-time output of sensor 2 when the running forward commands are executed at a low speed and a high speed. The boundary between the purple region and the pink region demonstrates the threshold voltage of the high-speed triggering. (c) The real-time output of sensor 1 when the car is triggered by the up-bending motion to move backward. (d) The real-time output of sensor 3 when the turning left commands are executed at a low speed and a high speed. (e) The real-time output of sensor 4 when the turning right commands are executed at a low speed and a high speed.

commands such as moving backward or turning left fast. Then this digital state signal will be transmitted from one wireless module to another one which is connected to the MCU for the car motor control. The corresponding signals from the four channels are depicted in Fig. 4(b–e). In Fig. 4(b), sensor 2 was triggered with index finger bending down at various angles, and hence two-level negative peak voltages were generated accordingly. At a low bending degree smaller than 60 degrees where the peak negative voltage is smaller than the set-up threshold voltage of 0.43 V in the region marked with light purple in Fig. 4(b), the toy car moves forward at a low velocity as shown in Fig. 4(f). While the index finger bends down at 90 degrees, the peak negative voltage exceeds the threshold voltage by at least 0.22 V and then commands the toy car run forward fast. Additionally, as mentioned in the characterization section the triboelectric outputs of the sensors increase with the moving speed of the finger, which is actually beneficial to the controlment. For most of the human motions including finger motions, the large applied force or the large bending angle is usually accompanied by a relatively high speed, and vice versa. Hence, while the glove-based interface is handled, the controlment can be further adjusted by the moving speed of the fingers in a straightforward way. In other words, to control the car run forward in low speed, one can bend the index finger down slowly and at a low degree; to command the toy car fast run forward, one can bend the index finger down at 90 degrees with a high velocity. By incorporating the finger motion speed to control the car, the operation accuracy could be further improved and simplified. As shown in Fig. 4(c), the sensor 1 that is defined as the backward control sensor is triggered whenever there is an up-bending motion at the MP joint of index finger, and the toy car will run reversely at a constant speed once a negative voltage is detected as shown in Fig. 4(g). To enable the car turn left and right, the triboelectric outputs of sensor 3 and sensor 4 are defined as the triggering signals for rotating left and right. Similar to the forward control, two speeds of the rotation are allowable by controlling the contact forces of the two sensors as well as the moving speed. Threshold voltages of 0.54 V and 0.59 V were set to differentiate the low-speed state and high-speed state of the sensor 3 and sensor 4. A video demo of the wireless car control can be found in Video S3 (Supporting Information). With a slight and gently touch, a low negative peak voltage will be generated as marked in the light purple region in Fig. 4(d–e) which will let the toy car start rotating slowly counterclockwise or clockwise.

Correspondingly, the car can be managed to rotate at a higher velocity with a slight increase on the applied force. Either the finger bending angle or the applied contact force of the index finger are intuitive to humans and easy to be controlled subconsciously due to the minimal involvement of moving muscles. Besides, the car movement could, in turn, serve as a visual feedback to the user that helps the user to quickly pick up the operation techniques of how to control its moving speed. This could further shorten the learning curve of this glove-based interface.

Supplementary material related to this article can be found online at doi:10.1016/j.nanoen.2019.01.091.

To expand the functionality of the glove-based control interface, we added two more contact-separation TENG sensors (sensor 5 and sensor 6) on another hand (left hand) on the same positions as the right hand. Together with these extra two sensors endowed with up-moving (sensor 5) and down moving (sensor 6) control capabilities as shown in Fig. S8, the expanded interface could realize a 3D control easily. Accordingly, the outputs of the six sensors were then used to control a drone fly in six directions. A video demo of wireless drone control can be found in Video S4 (Supporting Information). Song et al. reported a wearable force touch sensor array with a high sensitivity attached to the arm for drone control, yet only one threshold voltage is used to set up the “0” and “1” states in the control process which demonstrates that this two-state control signal is already good enough for drone controlling [64].

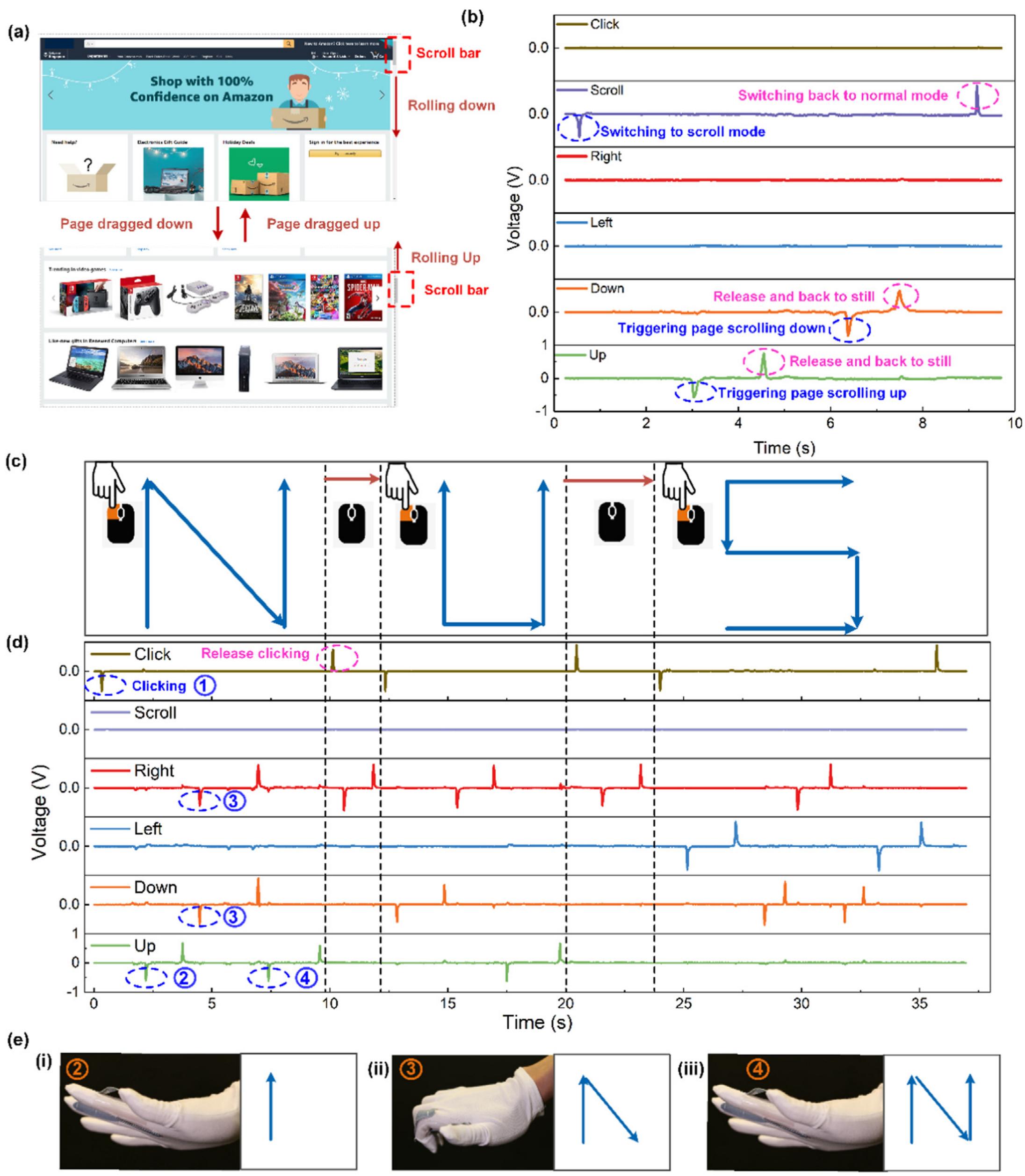

Fig. 5. Cursor control with the glove-based interface for online shopping and alphabet writing. (a) The screenshots of an online shopping website showing the page scrolled down and up. (b) Corresponding real-time outputs of the six sensors to control the website page scrolling down and up. (c) Schematic drawing demonstrating the moving trajectory of the cursor when the three characters are written on the screen. The highlighted mouse with a hand on top indicates the “click” sensor is triggered so as to start writing in the Paint application. (d) The real-time outputs of the six sensors during the whole control process to write “NUS” on the screen. The detailed steps while writing character “N” was highlighted with the blue circle labeled from 1 to 4 chronologically. (e) Photos of the corresponding hand gestures to write the character “N”. (i) Bending the index finger up to trigger the sensor 1 for cursor moving up. (ii) Bending the index finger down while contacting with the middle finger to trigger sensor 2 and sensor 3 at the same time for cursor moving diagonally down. (iii) Bending the index finger up again to command cursor move up.

Besides, the authors used six pixels of the force sensors to execute all the control commands, which is quite complex and not instinctive for the user to memorize all the gestures to be performed. Hence this glove-based control interface is more preferential due to the intuitive, simple, yet self-powered control schemes.

Supplementary material related to this article can be found online at doi:10.1016/j.nanoen.2019.01.091.

5. Cursor control

Besides of video games, toy cars, or drones, mouse or keyboard is also frequently-used control interfaces in our daily life. To demonstrate the glove-based interface as an alternative choice for cursor control in an electronic device, we connected the sensor outputs from the triboelectric sensors to a computer for online shopping and alphabets writing. Distinct to previously controlled entities, to endow this glove-based interface with full function of the mouse, two more contact separation sensors for the scroll mode switching and clicking are added onto another glove labeled as sensor 5 and sensor 6 as shown in Fig. S8. Similarly, the triboelectric signals from sensor 1–4 are defined as up, down, left, and right movement commands respectively. This expanded glove-based interface was then implemented to browse an online shopping website, add an item to the shopping basket, and finally proceed to check out. The real-time outputs of the six sensors when the page is controlled to scroll up and down are depicted in Fig. 5(b). Firstly, the sensor for the scroll mode switching was triggered by contacting the index finger with the thumb on the left hand, then bend up the index finger on the right hand to drag the website page up. Once a positive voltage is detected, the moving page stops at its current position. With the bending down of the index finger on the right hand, a negative voltage is generated from the sensor 2 and triggers the page to scroll down as shown in Fig. 5(a). When the page stays at the desired position and the operations on the cursor are needed, the index finger of the left hand can be controlled to separate from the side of thumb to generate a positive voltage for switching back to the normal mode as illustrated in Fig. 5(b). A video demo of online shopping through the glove-based interface can be found in Video S5 (Supporting Information).

Supplementary material related to this article can be found online at doi:10.1016/j.nanoen.2019.01.091.

Except for browsing a web page, one can also write or paint through the Paint application in the computer desktop. Here we successfully used the glove-based interface to write the alphabets "NUS" in the Paint application. The trajectory of the cursor when writing the three alphabets is depicted in Fig. 5(c), and the real-time outputs from the six channels are shown in Fig. 5(d). Firstly, the click sensor located at the left-hand glove was triggered to let the cursor become a pencil so as to enable write marked by a hand-clicked mouse in Fig. 5(c). Then the right hand performs different gestures to trigger sensors for different directional movements of the virtual pencil follows the same trajectories as shown in Fig. 5(c). After writing of each alphabet, the click sensor was released intentionally and the right sensor was then triggered to shift the cursor to where the start point of the next alphabet is. Before the start of writing the next alphabet with the four directional sensors, the click sensor was triggered to enable write function again. To make the whole process clearer, a detailed description of how to write the alphabet "N" was provided. Firstly, the index finger on the left hand was moved to contact with the middle finger to trigger the click function and the generated real-time output is marked as step one in Fig. 5(d). Then the right-hand index finger was bent up and stayed at this position for a short period to write a straight line as demonstrated in Fig. 5(e–i). The corresponding detected signal from sensor 1 is marked as step two in Fig. 5(d). As shown in Fig. 5(e-ii), the sensor 2 and sensor 3 were triggered at the same time through bending the index finger while touching with the middle finger to move the pencil in a diagonally downward direction in step three. Correspondingly, a negative voltage can be detected in both channel 2 and channel 3 as marked by the blue circle in Fig. 5(d). In step four, a same gesture with the step two was performed to finish the right straight line of "N" as demonstrated in Fig. 5(e-iii). Lastly, the sensor 6 staying at the contacted state during the whole period was released to stop the click function. Similarly, by combining with different hand gestures, other alphabets can also be written in the same way. A video demo of alphabet writing with the glove-based interface can be found in Video S6 (Supporting Information). Hence this glove-based interface works well as an alternative choice for the existing control interfaces to provide a simple and intuitive operation approach at situations where the rigid and bulky interfaces are in lack or hard to carry. Besides, it is also highly beneficial for people in some special situations where their hand may be too weak to operate the existing control interfaces.

Supplementary material related to this article can be found online at doi:10.1016/j.nanoen.2019.01.091.

6. Conclusion

In this study, a glove-based HMI is fabricated towards diversified applications ranging from 2D/3D control, game control, to cursor control in real/cyber space. A minimalist design based on the triboelectric nanogenerators in two configurations is proposed to balance the requirement on the full functionality and the easy to hands-on operation scheme. We have successfully demonstrated using the glove-based interface to control an aircraft in a shooting minigame. We have also controlled a real toy car run at all the directions on the ground wirelessly with different speeds through controlling the bending angles or the contacting forces. Similarly, a drone is also successfully controlled to fly and move in the 3D space with two more sensors embedded. With the additional sensors endowed with other defined functions, the expanded glove-based interface has also been demonstrated to mimic the same function of a mouse. Benefit from the minimalist design, this glove-based control interface could be easily produced in large scale due to the simplified device structure and its low-cost fabrication process. Looking forward, this wearable glove-based interface could be incorporated into more applications to provide a more intuitive, simple, yet power-compatible control method.

7. Experimental section

7.1. Fabrication of the glove-based interface

Firstly the as-purchased PEDOT:PSS solution was doped with 5 wt% DMSO solution to further improve its conductivity, and then the doped PEDOT:PSS solution was diluted by DI water to a weight percentage of 12.5% in the coating solution. The PEDOT:PSS functionalized textile was first fabricated with the dip coating method where the cotton textile was soaked in the PEDOT:PSS solution for 10 min for full absorption. Then the wet textile was put into an oven and baked for at least 30 min at 80 °C until it was fully dried. The next step was to prepare the silicone rubber thin films. After dispensing required amounts of Parts A and B of the EcoFlex™ 00-30 into a mixing container (1 A:1B by volume or weight), the blend was mixed thoroughly for 3 min, and then paint the mixed solution onto the plain glove at the desired locations followed by a 20-min baking at 70 °C for curing. Lastly, the PEDOT:PSS coated textiles are fixed on the glove by stitching.

7.2. Characterization of the textile-based sensors

Open-circuit voltage and short-circuit current measurement were conducted by connecting the output signal to a Keithley Electrometer (Model 6514), and the signals are displayed and recorded with a DSO-X3034A oscilloscope (Agilent). The speed of the finger movement is measured by a high-speed camera. To generate stretching motion with controllable speed, a linear motor connected to a programmable Arduino UNO was used.

Acknowledgements

This work was supported by HiFES Seed Funding-2017-01 grant (R-263-501-012-133) “Hybrid Integration of Flexible Power Source and Pressure Sensors” at the National University of Singapore; Faculty Research Committee (FRC) grant (R-263-000-B56-112) “Thermoelectric power generator (TEG) based selfpowered ECG plaster-System integration (Part 3)” at the National University of Singapore, Singapore. T.H. would like to appreciate the support from NUS Suzhou Research Institute (NUSRI) scholarship program for her Ph.D. study.

Appendix A. Supporting information

Supplementary data associated with this article can be found in the online version at doi:10.1016/j.nanoen.2019.01.091.

References

[1] S. Lim, D. Son, J. Kim, Y.B. Lee, J.K. Song, S. Choi, D.J. Lee, J.H. Kim, M. Lee, T. Hyeon, D.H. Kim, Transparent and stretchable interactive human machine interface based on patterned graphene heterostructures, Adv. Funct. Mater. 25 (2015) 375–383, https://doi.org/10.1002/adfm.201402987.

[2] A.P. Gerratt, H.O. Michaud, S.P. Lacour, Elastomeric electronic skin for prosthetic tactile sensation, Adv. Funct. Mater. 25 (2015) 2287–2295, https://doi.org/10.1002/adfm.201404365.

[3] S. Jung, J.H. Kim, J. Kim, S. Choi, J. Lee, I. Park, T. Hyeon, D.H. Kim, Reverse-micelle-induced porous pressure-sensitive rubber for wearable human-machine interfaces, Adv. Mater. 26 (2014) 4825–4830, https://doi.org/10.1002/adma.201401364.

[4] S. Takamatsu, T. Lonjaret, E. Ismailova, A. Masuda, T. Itoh, G.G. Malliaras, Wearable keyboard using conducting polymer electrodes on textiles, Adv. Mater. 28 (2016) 4485–4488, https://doi.org/10.1002/adma.201504249.

[5] J. Wang, G. Cai, S. Li, D. Gao, J. Xiong, P.S. Lee, Printable superelastic conductors with extreme stretchability and robust cycling endurance enabled by liquid-metal particles, Adv. Mater. 30 (2018) 1706157, https://doi.org/10.1002/adma.201706157.

[6] G. Cai, J. Wang, K. Qian, J. Chen, S. Li, P.S. Lee, Extremely stretchable strain sensors based on conductive self-healing dynamic cross-links hydrogels for human-motion detection, Adv. Sci. 4 (2017) 1600190, https://doi.org/10.1002/advs.201600190.

[7] J. Xu, S. Wang, G.N. Wang, C. Zhu, S. Luo, L. Jin, X. Gu, S. Chen, V.R. Feig, J.W.F. To, S. Rondeau-gagné, J. Park, B.C. Schroeder, C. Lu, J.Y. Oh, Y. Wang, Y. Kim, H. Yan, R. Sinclair, D. Zhou, G. Xue, B. Murmann, C. Linder, W. Cai, J.B. Tok, Highly stretchable polymer semiconductor films through the nanoconfinement effect, Science 355 (80) (2017) 59–64.

[8] S. Han, J. Kim, S.M. Won, Y. Ma, D. Kang, Z. Xie, K.T. Lee, H.U. Chung, A. Banks, S. Min, S.Y. Heo, C.R. Davies, J.W. Lee, C.H. Lee, B.H. Kim, K. Li, Y. Zhou, C. Wei, X. Feng, Y. Huang, J.A. Rogers, Battery-free, wireless sensors for full-body pressure and temperature mapping, Sci. Transl. Med. 10 (2018) eaan4950, https://doi.org/10.1126/scitranslmed.aan4950.

[9] H. Ouyang, J. Tian, G. Sun, Y. Zou, Z. Liu, H. Li, L. Zhao, B. Shi, Y. Fan, Y. Fan, Z.L. Wang, Z. Li, Self-powered pulse sensor for antidiastole of cardiovascular disease, Adv. Mater. 29 (2017) 1703456, https://doi.org/10.1002/adma.201703456.

[10] X. Wang, Y. Zhang, X. Zhang, Z. Huo, X. Li, M. Que, Z. Peng, H. Wang, C. Pan, A highly stretchable transparent self-powered triboelectric tactile sensor with metallized nanofibers for wearable electronics, Adv. Mater. 30 (2018) 1706738, https://doi.org/10.1002/adma.201706738.

[11] Y. Wang, Y. Wang, Y. Yang, Graphene–polymer nanocomposite-based redox-induced electricity for flexible self-powered strain sensors, Adv. Energy Mater. 8 (2018) 1800961, https://doi.org/10.1002/aenm.201800961.

[12] Q. Hua, J. Sun, H. Liu, R. Bao, R. Yu, J. Zhai, C. Pan, Z.L. Wang, Skin-inspired highly stretchable and conformable matrix networks for multifunctional sensing, Nat. Commun. 9 (2018) 244, https://doi.org/10.1038/s41467-017-02685-9.

[13] C. Wang, D. Hwang, Z. Yu, K. Takei, J. Park, T. Chen, B. Ma, A. Javey, User-interactive electronic skin for instantaneous pressure visualization, Nat. Mater. 12 (2013) 899–904, https://doi.org/10.1038/nmat3711.

[14] M. Ye, C. Yang, V. Stankovic, L. Stankovic, A. Kerr, A depth camera motion analysis framework for tele-rehabilitation: motion capture and person-centric kinematics analysis, IEEE J. Sel. Top. Signal Process. 10 (2016) 877–887, https://doi.org/10.1109/JSTSP.2016.2559446.

[15] J. Kim, J.H. Lee, H. Ryu, J.H. Lee, U. Khan, H. Kim, S.S. Kwak, S.W. Kim, High-performance piezoelectric, pyroelectric, and triboelectric nanogenerators based on P(VDF-TrFE) with controlled crystallinity and dipole alignment, Adv. Funct. Mater. 27 (2017) 1700702, https://doi.org/10.1002/adfm.201700702.

[16] H. Song, I. Karakurt, M. Wei, N. Liu, Y. Chu, J. Zhong, L. Lin, Lead iodide nanosheets for piezoelectric energy conversion and strain sensing, Nano Energy 49 (2018) 7–13, https://doi.org/10.1016/j.nanoen.2018.04.029.

[17] S.A. Han, T.-H. Kim, S.K. Kim, K.H. Lee, H.-J. Park, J.-H. Lee, S.-W. Kim, Point-defect-passivated MoS2 nanosheet-based high performance piezoelectric nanogenerator, Adv. Mater. 30 (2018) 1800342, https://doi.org/10.1002/adma.201800342.

[18] Z.L. Wang, Nanogenerators, self-powered systems, blue energy, piezotronics and piezo-phototronics – a recall on the original thoughts for coining these fields, Nano Energy 54 (2018) 477–483, https://doi.org/10.1016/j.nanoen.2018.09.068.

[19] D. Hu, M. Yao, Y. Fan, C. Ma, M. Fan, M. Liu, Strategies to achieve high performance piezoelectric nanogenerators, Nano Energy 55 (2019) 288–304, https://doi.org/10.1016/j.nanoen.2018.10.053.

[20] L. Feng, G. Liu, H. Guo, Q. Tang, X. Pu, J. Chen, X. Wang, Y. Xi, C. Hu, Hybridized nanogenerator based on honeycomb-like three electrodes for efficient ocean wave energy harvesting, Nano Energy 47 (2018) 217–223, https://doi.org/10.1016/j.nanoen.2018.02.042.

[21] X. Wang, Y. Yang, Effective energy storage from a hybridized electromagnetic-triboelectric nanogenerator, Nano Energy 32 (2017) 36–41, https://doi.org/10.1016/j.nanoen.2016.12.006.

[22] Q. Zheng, Y. Zou, Y. Zhang, Z. Liu, B. Shi, X. Wang, Y. Jin, H. Ouyang, Z. Li, Z.L. Wang, Biodegradable triboelectric nanogenerator as a life-time designed implantable power source, Sci. Adv. 2 (2016) e1501478, https://doi.org/10.1126/sciadv.1501478.

[23] J. Xiong, M.F. Lin, J. Wang, S.L. Gaw, K. Parida, P.S. Lee, Wearable all-fabric-based triboelectric generator for water energy harvesting, Adv. Energy Mater. 7 (2017) 1701243, https://doi.org/10.1002/aenm.201701243.

[24] Q. Shi, T. He, C. Lee, More Than Energy Harvesting - Combining Triboelectric Nanogenerator and Flexible Electronics Technology for Enabling Novel Micro-/Nano-Systems, Nano Energy 57 (2019) 851–871, https://doi.org/10.1016/j.nanoen.2019.01.002.

[25] L. Dhakar, P. Pitchappa, F. Eng, H. Tay, C. Lee, An intelligent skin based self-powered finger motion sensor integrated with triboelectric nanogenerator, Nano Energy 19 (2016) 532–540, https://doi.org/10.1016/j.nanoen.2015.04.020.

[26] T. Chen, M. Zhao, Q. Shi, Z. Yang, H. Liu, L. Sun, J. Ouyang, C. Lee, Novel augmented reality interface using a self-powered triboelectric based virtual reality 3D-control sensor, Nano Energy 51 (2018) 162–172, https://doi.org/10.1016/j.nanoen.2018.06.022.

[27] G. Shi, Z. Zhao, J.H. Pai, I. Lee, L. Zhang, C. Stevenson, K. Ishara, R. Zhang, H. Zhu, J. Ma, Highly sensitive, wearable, durable strain sensors and stretchable conductors using graphene/silicon rubber composites, Adv. Funct. Mater. 26 (2016) 7614–7625, https://doi.org/10.1002/adfm.201602619.

[28] S.B. Jeon, S.J. Park, W.G. Kim, I.W. Tcho, I.K. Jin, J.K. Han, D. Kim, Y.K. Choi, Self-powered wearable keyboard with fabric based triboelectric nanogenerator, Nano Energy 53 (2018) 596–603, https://doi.org/10.1016/j.nanoen.2018.09.024.

[29] Y.C. Lai, J. Deng, S.L. Zhang, S. Niu, H. Guo, Z.L. Wang, Single-thread-based wearable and highly stretchable triboelectric nanogenerators and their applications in cloth-based self-powered human-interactive and biomedical sensing, Adv. Funct. Mater. 27 (2017) 1604462, https://doi.org/10.1002/adfm.201604462.

[30] S. Chen, Z. Lou, D. Chen, K. Jiang, G. Shen, Polymer-enhanced highly stretchable conductive fiber strain sensor used for electronic data gloves, Adv. Mater. Technol. 1 (2016) 1600136, https://doi.org/10.1002/admt.201600136.

[31] T. He, Q. Shi, H. Wang, F. Wen, T. Chen, J. Ouyang, C. Lee, Beyond energy harvesting-multi-functional triboelectric nanosensors on a textile, Nano Enegy 57 (2016) 338–352, https://doi.org/10.1016/j.nanoen.2018.12.032.

[32] J. Chen, H. Guo, X. Pu, X. Wang, Y. Xi, C. Hu, Traditional weaving craft for one-piece self-charging power textile for wearable electronics, Nano Energy 50 (2018) 536–543, https://doi.org/10.1016/j.nanoen.2018.06.009.

[33] A. Yu, X. Pu, R. Wen, M. Liu, T. Zhou, K. Zhang, Y. Zhang, J. Zhai, W. Hu, Z.L. Wang, Core-shell-yarn-based triboelectric nanogenerator textiles as power cloths, ACS Nano 11 (2017) 12764–12771, https://doi.org/10.1021/acsnano.7b07534.

[34] Y.T. Jao, P.K. Yang, C.M. Chiu, Y.J. Lin, S.W. Chen, D. Choi, Z.H. Lin, A textile-based triboelectric nanogenerator with humidity-resistant output characteristic and its applications in self-powered healthcare sensors, Nano Energy 50 (2018) 513–520, https://doi.org/10.1016/j.nanoen.2018.05.071.

[35] M. Tessarolo, I. Gualandi, B. Fraboni, Recent progress in wearable fully textile chemical sensors, Adv. Mater. Technol. 3 (2018) 1700310, https://doi.org/10.1002/admt.201700310.

[36] M. Liu, X. Pu, C. Jiang, T. Liu, X. Huang, L. Chen, C. Du, J. Sun, W. Hu, Z.L. Wang, Large-area all-textile pressure sensors for monitoring human motion and physiological signals, Adv. Mater. 29 (2017) 1703700, https://doi.org/10.1002/adma.201703700.

[37] R. Cao, X. Pu, X. Du, W. Yang, J. Wang, H. Guo, S. Zhao, Z. Yuan, C. Zhang, C. Li, Z.L. Wang, Screen-printed washable electronic textiles as self-powered touch/gesture tribo-sensors for intelligent human − machine interaction, ACS Nano 12 (2018) 5190–5196, https://doi.org/10.1021/acsnano.8b02477.

[38] L. Li, Y. Bai, L. Li, S. Wang, T. Zhang, A superhydrophobic smart coating for flexible and wearable sensing electronics, Adv. Mater. 29 (2017) 1702517, https://doi.org/10.1002/adma.201702517.

[39] Z. Chen, Z. Wang, X. Li, Y. Lin, N. Luo, M. Long, N. Zhao, J. Bin Xu, Flexible piezoelectric-induced pressure sensors for static measurements based on nanowires/graphene heterostructures, ACS Nano 11 (2017) 4507–4513, https://doi.org/10.1021/acsnano.6b08027.

[40] H.B. Song, Lead iodide nanosheets for piezoelectric energy conversion and strain sensing, Nano Energy 49 (2018) 7–13.

[41] L. Jin, S. Ma, W. Deng, C. Yan, T. Yang, X. Chu, G. Tian, Polarization-free high-crystallization β-PVDF piezoelectric nanogenerator toward self-powered 3D acceleration sensor, Nano Energy 50 (2018) 632–638, https://doi.org/10.1016/j.

nanoen.2018.05.068.
[42] C. Yan, W. Deng, L. Jin, T. Yang, Z. Wang, X. Chu, H. Su, J. Chen, W. Yang, Epidermis-inspired ultrathin 3D cellular sensor array for self-powered biomedical monitoring, ACS Appl. Mater. Interfaces 10 (2018) 41070–41075, https://doi.org/10.1021/acsami.8b14514.
[43] W. Deng, T. Yang, L. Jin, C. Yan, H. Huang, X. Chu, Z. Wang, Cowpea-structured PVDF/ZnO nano fibers based flexible self-powered piezoelectric bending motion sensor towards remote control of gestures, Nano Energy 55 (2019) 516–525.
[44] X. Gao, J. Wu, Y. Yu, Z. Chu, H. Shi, S. Dong, Giant piezoelectric coefficients in relaxor piezoelectric ceramic PNN-PZT for vibration energy harvesting, Adv. Funct. Mater. 28 (2018) 1706895, https://doi.org/10.1002/adfm.201706895.
[45] Y.B. Lee, J.K. Han, S. Noothongkaew, S.K. Kim, W. Song, S. Myung, S.S. Lee, J. Lim, S.D. Bu, K.S. An, Toward arbitrary-direction energy harvesting through flexible piezoelectric nanogenerators using perovskite PbTiO3 nanotube arrays, Adv. Mater. 29 (2017) 1604500, https://doi.org/10.1002/adma.201604500.
[46] K. Shi, B. Sun, X. Huang, P. Jiang, Synergistic effect of graphene nanosheet and BaTiO3 nanoparticles on performance enhancement of electrospun PVDF nanofiber mat for flexible piezoelectric nanogenerators, Nano Energy 52 (2018) 153–162, https://doi.org/10.1016/j.nanoen.2018.07.053.
[47] K. Zhao, Y. Yang, X. Liu, Z.L. Wang, Triboelectrification-enabled self-charging lithium-ion batteries, Adv. Energy Mater. 7 (2017) 1700103, https://doi.org/10.1002/aenm.201700103.
[48] H. Feng, C. Zhao, P. Tan, R. Liu, X. Chen, Z. Li, Nanogenerator for biomedical applications, Adv. Healthc. Mater. 7 (2018) 1701298, https://doi.org/10.1002/adhm.201701298.
[49] Z. Yuan, N. Li, X. Du, C. Wang, S. Zhao, Y. Liu, Self-powered electrospinning system driven by a triboelectric nanogenerator, ACS Nano 11 (2017) 10439–10445, https://doi.org/10.1021/acsnano.7b05626.
[50] S.W. Chen, X. Cao, N. Wang, L. Ma, H.R. Zhu, M. Willander, Y. Jie, Z.L. Wang, An ultrathin flexible single-electrode triboelectric-nanogenerator for mechanical energy harvesting and instantaneous force sensing, Adv. Energy Mater. 7 (2017) 1601255, https://doi.org/10.1002/aenm.201601255.
[51] G. Gao, B. Wan, X. Liu, Q. Sun, X. Yang, L. Wang, C. Pan, Z.L. Wang, Tunable tribotronic dual-gate logic devices based on 2D MoS2 and black phosphorus, Adv. Mater. 30 (2018) 1705088, https://doi.org/10.1002/adma.201705088.
[52] X. Liu, K. Zhao, Z.L. Wang, Y. Yang, Unity convoluted design of solid li-ion battery and triboelectric nanogenerator for self-powered wearable electronics, Adv. Energy Mater. 7 (2017) 1701629, https://doi.org/10.1002/aenm.201701629.
[53] W. Jiang, H. Li, Z. Liu, Z. Li, J. Tian, B. Shi, Y. Zou, H. Ouyang, C. Zhao, L. Zhao, R. Sun, H. Zheng, Y. Fan, Z.L. Wang, Z. Li, Fully bioabsorbable natural-materials-based triboelectric nanogenerators, Adv. Mater. 30 (2018) 1801895, https://doi.org/10.1002/adma.201801895.
[54] B. Chen, Y. Yang, Z.L. Wang, Scavenging wind energy by triboelectric nanogenerators, Adv. Energy Mater. 8 (2018) 1702649, https://doi.org/10.1002/aenm.201702649.
[55] J. Chen, X. Pu, H. Guo, Q. Tang, L. Feng, X. Wang, C. Hu, A self-powered 2D barcode recognition system based on sliding mode triboelectric nanogenerator for personal identification, Nano Energy 43 (2018) 253–258, https://doi.org/10.1016/j.nanoen.2017.11.028.
[56] Q. Shi, H. Wang, T. Wang, C. Lee, Self-powered liquid triboelectric microfluidic sensor for pressure sensing and finger motion monitoring applications, Nano Energy 30 (2016) 450–459, https://doi.org/10.1016/j.nanoen.2016.10.046.
[57] H. Shi, C. Liu, Q. Jiang, J. Xu, Effective approaches to improve the electrical conductivity of PEDOT:PSS: a review, Adv. Electron. Mater. 1 (2015) 1500017, https://doi.org/10.1002/aelm.201500017.
[58] B.C.K. Tee, J. Ouyang, Soft Electronically Functional Polymeric Composite Materials for a Flexible and Stretchable Digital Future, Adv. Mater. 30 (2018) 1802560, https://doi.org/10.1002/adma.201802560.
[59] X. Pu, L. Li, M. Liu, C. Jiang, C. Du, Z. Zhao, W. Hu, Z.L. Wang, Wearable self-charging power textile based on flexible yarn supercapacitors and fabric nanogenerators, Adv. Mater. 28 (2016) 98–105, https://doi.org/10.1002/adma.201504403.
[60] Z. Yang, Y. Pang, X. Han, Y. Yang, J. Ling, M. Jian, Y. Zhang, Y. Yang, T. Ren, Graphene textile strain sensor with negative, ACS Nano 12 (2018) 9134–9141, https://doi.org/10.1021/acsnano.8b03391.
[61] B.Y. Liang, D. Sias, P.J. Chen, S. Tawfick, Tough nano-architectured conductive textile made by capillary splicing of carbon nanotubes, Adv. Energy Mater. 19 (2017) 1600845, https://doi.org/10.1002/adem.201600845.
[62] Y. Ding, M.A. Invernale, G.A. Sotzing, Conductivity trends of pedot-pss impregnated fabric and the effect of conductivity on electrochromic textile, ACS Appl. Mater. Interfaces 2 (2010) 1588–1593, https://doi.org/10.1021/am100036n.
[63] X. Pu, H. Guo, Q. Tang, J. Chen, L. Feng, G. Liu, X. Wang, Y. Xi, C. Hu, Z. Lin, Rotation sensing and gesture control of a robot joint via triboelectric quantization sensor, Nano Energy 54 (2018) 453–460, https://doi.org/10.1016/j.nanoen.2018.10.044.
[64] J.K. Song, D. Son, J. Kim, Y.J. Yoo, G.J. Lee, L. Wang, M.K. Choi, J. Yang, M. Lee, K. Do, J.H. Koo, N. Lu, J.H. Kim, T. Hyeon, Y.M. Song, D.H. Kim, Wearable force touch sensor array using a flexible and transparent electrode, Adv. Funct. Mater. 27 (2017) 1605286, https://doi.org/10.1002/adfm.201605286.

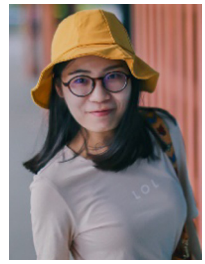

Tianyiyi He received her B.Eng. degree from the School of Microelectronics and Solid-state Electronics at the University of Electronic Science and Technology of China (UESTC), Chengdu, China, in 2016. She is now a Ph.D. candidate in the Department of Electrical and Computer Engineering, National University of Singapore. Her research interests include energy harvesters, triboelectric nanogenerator, thermoelectric energy harvester, and self-powered sensors.

Zhongda Sun received his B.Eng. degree from the School of Electronic and Information at the Soochow University, Suzhou, China, in 2018. He is now a Master student in the Department of Electrical and Computer Engineering, National University of Singapore. His research interests include self-powered wearable sensors, energy harvesters and triboelectric nanogenerator.

Qiongfeng Shi received his B.Eng. degree from the Department of Electronic Engineering and Information Science, University of Science and Technology of China (USTC) in 2012, and received his Ph.D. degree from the Department of Electrical and Computer Engineering, National University of Singapore (NUS) in 2018. He is currently a Research Fellow in the Department of Electrical and Computer Engineering, National University of Singapore. His research interests include energy harvesters, triboelectric nanogenerator, self-powered sensors, and wearable/implantable electronics.

Minglu Zhu received his B.Bus. degree in Business Administration from the School of Business at State University of Bangladesh, Dhaka, Bangladesh, in 2010, and B.Sc. degree in Materials Science and Engineering from the School of Materials Science and Engineering at University of Illinois at Urbana-Champaign, Illinois, United States, in 2014. He is now a Ph.D. student at the Department of Electrical & Computer Engineering, NUS. His research interests focus mainly on MEMS based energy harvesters and self-powered sensors.

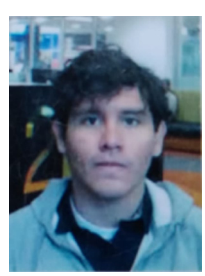

David Vera Anaya received his Bachelor degree in Electronic Engineering from the Department of Electrical and Electronic Engineering at North University "Universidad Del Norte" of Barranquilla, Colombia in 2016. He is currently pursuing his Ph.D degree with the Department of Electrical and Computer Systems at Monash University in Melbourne, Australia. His Research interests include energy harvesting systems targeted to biomedical applications, triboelectric nanogenerators, wireless sensor networks and wearable and self-powered sensors.

Mengya Xu received her B.Eng. degree from the School of Electronic and Information Engineering, Soochow University, Suzhou, China, in 2018. She is now a M.Sc. candidate in the Department of Electrical and Computer Engineering, National University of Singapore. Her research interests include energy harvesters, triboelectric nanogenerator, wearable/implantable electronics and self-powered sensors.

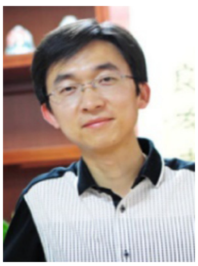

Tao Chen received the B.Sc. degree in Mechanical Design, Manufacturing and Automation, M.Sc. degree in Mechatronic Engineering, and Ph.D. degree in Mechatronic Engineering from Harbin Institute of Technology, Harbin, China, in 2004, 2006, and 2010, respectively. He is a visiting scholar in National University of Singapore in 2018. He is currently an associate professor at Soochow University, Suzhou, China. His main research interests include MEMS, sensors, and actuators.

Mehmet Rasit Yuce received the M.S. degree in electrical and computer engineering from the University of Florida, Gainesville, FL, in 2001, and the Ph.D. degree in electrical and computer engineering from North Carolina State University, Raleigh, NC, in 2004. In 2011, he joined the Department of Electrical and Computer Systems Engineering, Monash University, Australia. His research interests include wearable devices, wireless implantable telemetry, wireless body area network, biosensors, and integrated circuit technology dealing with digital, analog, and radio frequency circuit designs for wireless, biomedical, and RF applications. He has published more than 100 technical articles in the above areas.

Aaron Voon-Yew Thean received his B.Sc. (Highest Honors & Graduated as Edmund J. James' Scholar), M.Sc., and Ph.D. degrees in Electrical Engineering, University of Illinois at Champaign-Urbana, USA. Currently, he is a Professor of Electrical and Computer Engineering at the National University of Singapore. He is also a consulting Fellow to IMEC, a Nano-electronic Research Center, based in Belgium. He has published over 300 technical papers and holds more than 50 U.S. patents for inventions in the field of advanced electronics.

Chengkuo Lee received his Ph.D. degree in Precision engineering from The University of Tokyo in 1996. Currently, he is the director of Center for Intelligent Sensors and MEMS, and an Associate Professor in the Department of Electrical and Computer Engineering, National University of Singapore, Singapore. In 2001, he cofounded Asia Pacific Microsystems, Inc., where he was the Vice President. From 2006 to 2009, he was a Senior Member of the Technical Staff at the Institute of Microelectronics, A-STAR, Singapore. He has contributed to more than 300 international conference papers and extended abstracts and 270 peer-reviewed international journal articles.